Consequences of Coronal Mass Ejections in the Heliosphere

N. Gopalswamy

NASA Goddard Space Flight Center, Greenbelt, MD 20771, USA

e-mail: gopals@ssedmail.gsfc.nasa.gov

Coronal mass ejections (CMEs) are the most energetic events in the heliosphere. They carry large amounts of coronal magnetic fields and plasma with them and drive large-scale interplanetary shocks. The CMEs and shock have significant consequences at various locations in the heliosphere, including the production of intense geomagnetic storms and large energetic particle events. CMEs form merged interaction regions in the heliosphere, which act as magnetic barriers for the galactic cosmic rays entering the heliosphere. After a brief summary of the observed properties of CMEs at the Sun, I discuss the properties of the interplanetary CMEs (ICMEs) and their connection to shocks, radio bursts, solar energetic particles and the modulation of galactic cosmic rays.

Introduction

The mass emission from the Sun in the form of solar wind defines the heliosphere. The heliospheric plasma originates from the hot corona of the Sun, whether it is the solar wind or the coronal mass ejections (CMEs). While the solar wind speed roughly varies by a factor of 2 depending upon the source region (coronal hole or quiet Sun), CMEs have a much wider range of speeds. Most of the large scale variability in the heliosphere can be attributed to these two types of mass emissions from the Sun. Energetic particles is the third component, mostly related to shocks driven by CMEs or by corotating interaction regions (CIRs) formed by the interaction of fast and slow solar wind. In addition to these internal components, mass comes from outside the heliosphere in the form of neutral atoms and galactic cosmic rays. The neutral atoms interact with the solar wind, get ionized and become the so-called anomalous cosmic rays. Galactic cosmic rays also interact with CMEs and CIRs and their intensity gets modulated. The mass emissions also interact with one another and impact the planetary atmospheres in the solar system. This paper focuses on the CME component and highlights their consequences in the heliosphere.

Basic properties of coronal mass ejections

CMEs have been studied extensively since their discovery in the early 1970s (see [1] for a recent review). The statistical properties of CMEs observed by the Solar and Heliospheric Observatory (SOHO) Mission's Large Angle and Spectrometric Coronagraph (LASCO [2]) can be summarized as follows [3]:

(1) the CME speed varies over two orders of magnitude from ~20 km/s to more than 3000 km/s, with an average value of 482 km/s. Out of the 9744 CMEs for which speeds could be measured, there are only 4 events with speeds < 30 km/s and only 2 with speeds exceeding 3000 km/s. The highest linear speed recorded by SOHO was ~3387 km/s for the 2004 November 10 CME. Only ~0.01% of CMEs had speeds exceeding 2500 km/s (see Fig. 1).

(2) The CME width ranges from <5 deg to 360 deg. CMEs with an apparent width of 360 deg. are known as halo CMEs because of they appear to surround the occulting disk of the coronagraph in the sky plane [4]. Halo CMEs were considered as a novelty in the pre-SOHO era, but now they are routinely observed [3]. The average width, determined only for CMEs narrower than 120 degrees, is ~47 deg (the actual width of halo CMEs is unknown). Wide CMEs (width >120 deg) and full halo CMEs (width = 360 deg) amount to ~11% and ~3.5%, respectively of all CMEs. The last bin in the width distribution (Fig. 1) gives the halo CMEs. Widths down to 2 deg were measured, but many such narrow CMEs might have been missed. In fact the narrowest CMEs must merge with features of the solar wind.

(3) CME acceleration within the coronagraphic field of view is generally speed-dependent. CMEs with the above-average speeds decelerate due to coronal drag [5-7], while those with speeds well below the average accelerate. CMEs with speeds close to the average speed do not have observable acceleration.

(4) Each CME represents a mass loss of ~4.4x10^{14} g on the average from the Sun. CME mass ranges from a few times 10^{12} g to more than 10^{16} g. Wider CMEs generally have a greater mass content (see Fig. 2). The corresponding kinetic energies range from ~10^{27} erg to more than 10^{32} erg, with an average value of 5.4x10^{29} erg.

(5) The average daily CME rate significantly increases from solar minimum to maximum (see Fig. 3). The rate averaged over Carrington rotation periods ranges from <0.5 per day (solar minimum) to >6 CMEs per day (solar maximum). High-latitude (>60 deg) CMEs contribute to the CME rate significantly during solar maximum. The high-latitude CME activity disappears around the time of polarity reversal in each pole of the Sun [8].

(6) The average speed of CMEs is also solar-cycle dependent, increasing by a factor of 2 from ~250 km/s during solar minimum to ~550 km/s during solar maximum.

(7) CMEs are multithermal plasmas containing coronal material at a temperature of ~ a few x10^6 K and prominence material at ~8000 K in the core.

(8) CMEs originate from closed field regions on the Sun, which are active regions, filament regions, and transequatorial interconnecting regions.

CMEs do not fall back to the Sun, so most of them enter into the interplanetary medium. However, part of the inner core often falls back along magnetic field lines, as observed in H-alpha [9], white light [10] and microwaves [11]. Not all CMEs are seen as distinct perturbations far away from the Sun and many CMEs

fade within the coronagraph field of view. Fig. 1 shows the speed and width distribution of CMEs which can be tracked up to and beyond 20 R⊙. Such CMEs constitute ~20% of all CMEs. The average speed (~700 km/s) and width (~65 deg, excluding halos) of these CMEs well exceed the corresponding values of the general population. Clearly, the CMEs observed at 20 R⊙ and beyond are likely to travel far into the heliosphere.
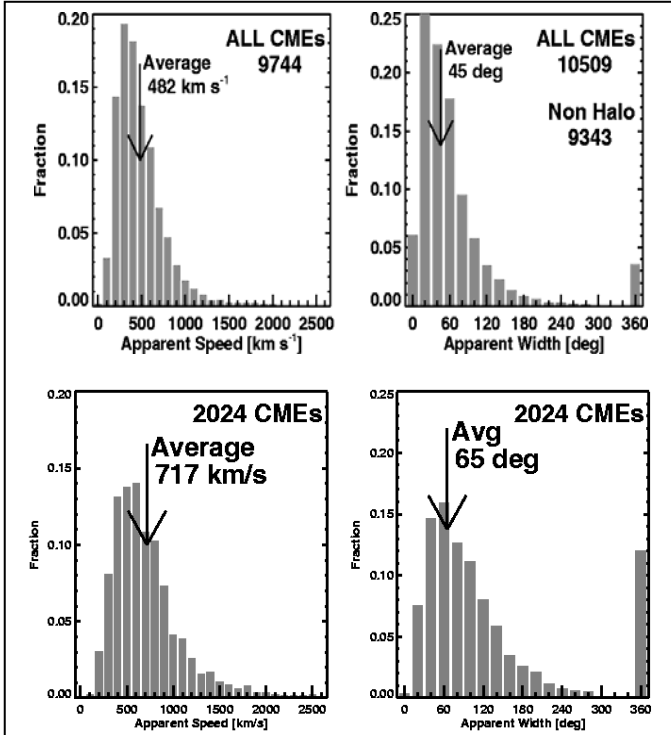

Fig. 1. Speed (left) and width (right) of all CMEs (top) and of those observed beyond 20 R⊙ (bottom) observed from 1996 until the end of 2005. Speed could be measured only for 9744 of the 10509 CMEs detected by SOHO. In the width distribution, the non-halo CMEs are those with width< 120 deg. The average values of the distributions are shown in the figure.
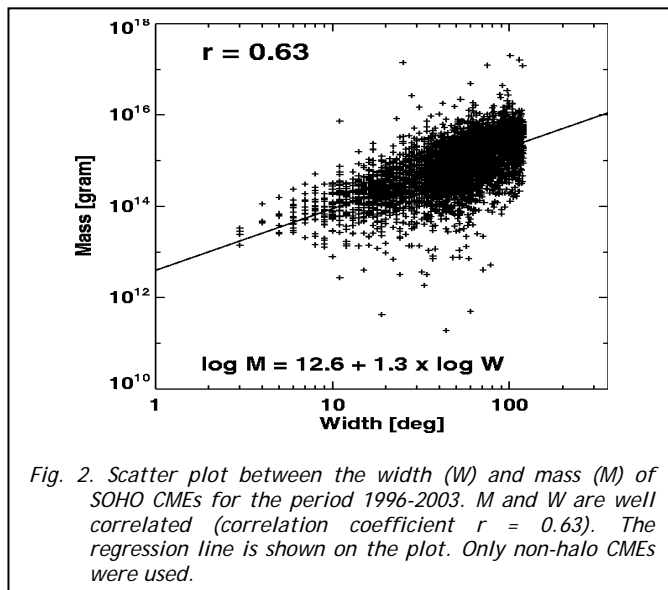

Fig. 2. Scatter plot between the width (W) and mass (M) of SOHO CMEs for the period 1996-2003. M and W are well correlated (correlation coefficient r = 0.63). The regression line is shown on the plot. Only non-halo CMEs were used.

CMEs have several consequences in the heliosphere: 1) The plasma and magnetic field of CMEs propagate into the heliosphere and are detected *in situ*. CMEs can also impact planetary atmospheres. CMEs impinging on Earth's magnetosphere can cause severe geomagnetic storms; such CMEs are known as geoeffective CMEs. 2) When the speed of CMEs relative to the ambient medium is higher than the local characteristic speeds (Alfven or fast mode speed) they can drive MHD shocks. The shocks can be tracked in the inner heliosphere using long-wavelength radio bursts from electrons accelerated at the shock front. The shocks can also be detected by *in situ* observations. 3) CME-driven shocks accelerate ions to very high energies, which are detected by spacecraft from locations magnetically well connected to the shock [12]; the underlying CMEs are considered as SEPeffective.
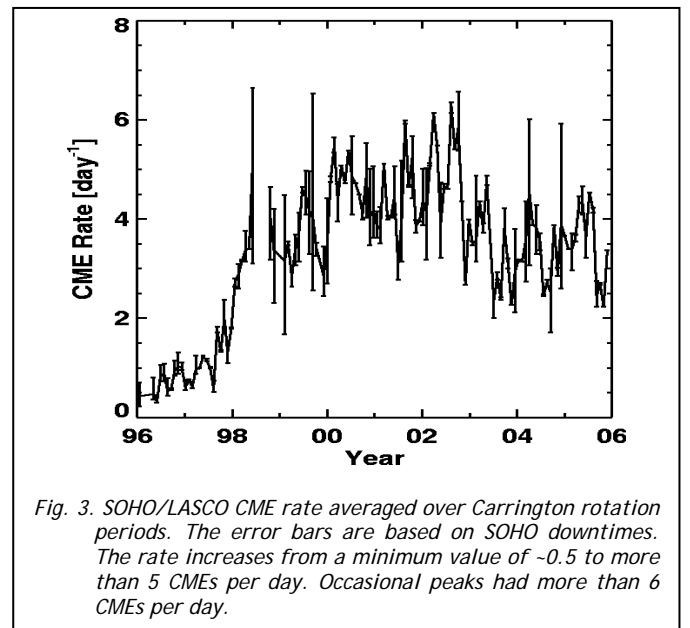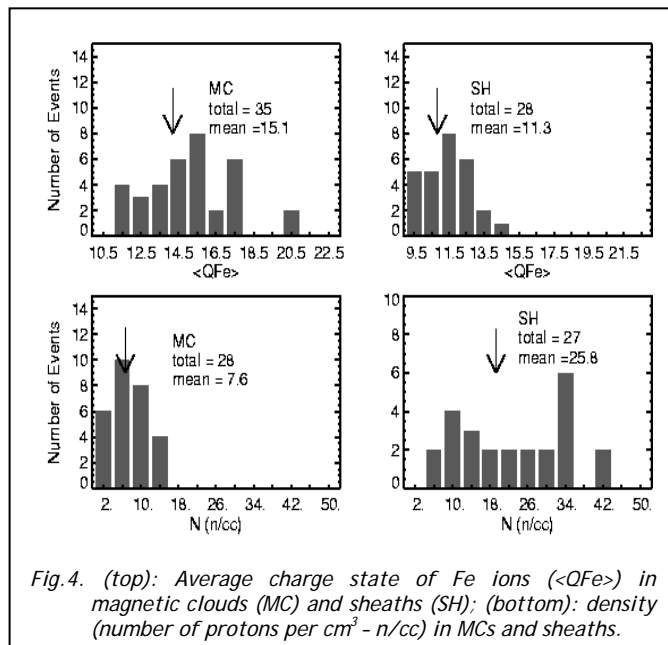

Fig. 3. SOHO/LASCO CME rate averaged over Carrington rotation periods. The error bars are based on SOHO downtimes. The rate increases from a minimum value of ~0.5 to more than 5 CMEs per day. Occasional peaks had more than 6 CMEs per day.

Coronal mass ejections in the IP medium

CMEs observed in the interplanetary (IP) medium are known as IP CMEs or ICMEs. Other names such as driver gas, ejecta, magnetic clouds (MCs) and flux ropes are also used. While CMEs near the Sun are observed as a density signature (photospheric light Thomson-scattered by coronal electrons), ICMEs are observed using many different signatures [13, 14]. The term "driver gas" has been used to denote the material behind IP shocks, which acts as a piston to drive the shocks. Such material contains enhanced helium abundance, which has along been used as a signature to identify ICMEs [15, 16]. "Ejecta" is the general term, like ICME, used to denote material coming from the Sun, which is distinct from the solar wind in terms of density, temperature or magnetic field. MC denotes ICMEs with enhanced magnetic field, smooth rotation of the field, and low plasma beta within the ICME [17]. Flux ropes are the same as MCs, but with a less restrictive condition on the plasma beta. The term "cloud-like" is used as a slight generalization of magnetic clouds, relaxing the smooth rotation aspect [18]. ICME flux ropes are connected to the Sun at both the ends, as inferred from the bidirectional flux of electrons, ions and

energetic particles [14]. Such a closed field structure has also been inferred from multi-spacecraft observations of an ICME [19]. A closed field structure is also consistent with the origin of CMEs from closed field regions on the Sun, where the presence of flux ropes have been inferred from coronal cavities in eclipse pictures and EUV and X-ray images [20].

One of the consequences of the closed field structure is the low temperature and density inside MCs. When the flux rope expands from near the Sun, the density and temperature decrease. On the other hand, the density and temperature are higher in the compressed sheath region between the flux rope and the shock ahead. Fig.4 shows that the average density inside MCs is ~8 cm^{-3}, while the density in the sheath region is higher by a factor of ~3. The charge state and composition of heavy elements inside MCs is also different from the solar wind [21-23]. Fig. 4 shows that the distribution of average ion charge state (<QFe> ~15.1) inside MCs is substantially higher than that (11.3) in the shock sheath, not too different from the solar wind value (~10). This suggests that the sheath region may not contain closed magnetic field structure. The enhanced charge state requires high temperatures at the source near the Sun. CMEs are associated with eruptive flares, so the heated plasma in the flaring region has to enter into the flux rope as it lifts off. A reasonable correlation between flare size and the charge state enhancement has been confirmed recently [23]. Connection to eruptive prominences is also found in ICMEs: unusually low charge states found in the bottom of MCs at 1 AU are indicative of the cool prominence material. The 1-AU prominence events are extremely rare, probably hard to detect due to their small overall size [24].

Fig.4. (top): Average charge state of Fe ions (<QFe>) in magnetic clouds (MC) and sheaths (SH); (bottom): density (number of protons per cm³ – n/cc) in MCs and sheaths.

Initially it was thought that only about a third of all ICMEs have MC structure [25], but it turns out that this fraction changes with solar cycle [26]. However, the ICME rate itself consistently follows the CME rate [27, 28]. MCs and non-cloud ejecta behave similarly in a number of ways, except that their solar sources are slightly different: the non-cloud ejecta originate from slightly larger central meridian distance on the Sun than the cloud events [28], suggesting the possibility that an ICME may be a cloud or non-cloud depending on the vantage point of the observer. The center-to-limb variation of the ionic charge states in ICMEs [23] may be supportive of this picture. This is not proven, but a useful hypothesis used by most modelers of ICMEs.

Statistical properties of magnetic clouds, reviewed recently [29] can be summarized as follows: the average speed of MCs is 420 km/s and the duration is 27 h. The diameter of the cloud at 1 AU is 0.28 AU and the average axial field strength is 17.7 G. These values were obtained for MCs from the pre-Wind era (1967-1982 by IMP, ISEE 3, and Helios 1) and Wind era (1995-1998). From Wind observations obtained until the end of 2003 it was found [28] that the speed (478 km/s), duration (20.9 h) and magnetic field strength (16.9 G), were not too different from earlier values reported in [29]. In [28], the speed corresponds to the leading edge and the magnetic field strength is the maximum value within the cloud interval.

ICMEs have been observed up beyond 50 AU by Voyager-2 [30]. A compilation of ICMEs from many spacecraft (Helios-1 and 2, Pioneer Venus Orbiter, ACE, and Ulysses) over a heliocentric distance (R) of 0.3 to 5.4 AU showed that the ICME rate roughly followed the solar activity cycle [31] with a rapid fall off of density (~R$^{-2.4}$) and magnetic field (~R$^{-1.5}$) inside the ICMEs than in the solar wind. The temperature, while smaller than in the solar wind, fell less rapidly (~R$^{-0.7}$).

CMEs and ICMEs

The close connection between ICMEs and CMEs was well established in the early 1980s [16, 17, 32]. For a subset of ICMEs with overlapping white-light observations, it was found that the CME and ICME speeds are correlated [33].

The distribution of ICME speeds was found to be narrower and closer to the solar wind speed compared to the distribution of CMEs near the Sun [34]. ICMEs, irrespective of their magnetic field structure, need to originate close to the disk center in order to be intercepted by spacecraft along the Sun-Earth line [34]. Such CMEs often appear as halos in white light observations, with distinct IP counterparts near Earth [35], except when successive CMEs merge [36]. SOHO has observed hundreds of halos, which have helped in establishing the connection between CMEs and ICMEs. However, details remain to be worked out as to how the substructures of CMEs and ICMEs map to each other. A working hypothesis [37] is to relate the features observed at 1 AU as *shock + sheath + magnetic cloud* to the near-Sun observations as *shock + CME frontal structure + cavity*. In addition to these three parts, a prominence core is often seen near the Sun, which is observed at 1 AU only extremely rarely [38]. Unfortunately, halo CMEs do not show these substructures very well because of the occulting disk employed by coronagraphs. Observations from the soon-to-be-launched STEREO mission are likely to help make progress on this issue. It is ironic that the magnetic field in ICMEs is a key measured physical

quantity, which is poorly known in the corresponding CMEs near the Sun due to lack of reliable measurements of magnetic fields in the corona.

It takes about 1-4 days for a CME to reach 1 AU [34]. It might take at least 6 months for them to reach the outer heliosphere [39]. CMEs have to interact with the coronal medium or solar wind through which they propagate. This interaction has been described by aerodynamic drag [40]. The change in CME speeds as they propagate through the corona and IP medium has been quantified in terms of an interplanetary acceleration [34]. The acceleration a (m/s^2) depends on the initial CME speed (V km/s) according to: $a = -0.0054$ ($V - 406$). Thus a 200 km/s CME would have an effective acceleration of ~1 m/s^2 while a 2500 km/s would have a deceleration of ~11 m/s^2. However, CMEs with V ~406 km/s would have no acceleration. The critical speed $V = 406$ km/s is close to the solar wind speed. This acceleration can be used to predict the speed and arrival time of CMEs and shocks at a destination in the heliosphere [41-42].

Merged interaction regions (MIRs) happen when successive CMEs merge among themselves and/or with interaction regions between solar wind streams. MIRs have been observed beyond 1 AU [43], but they form occasionally at 1 AU [44].

ICMEs and geomagnetic storms

The impact of ICMEs on planets depends on the magnetic nature of the planet. For example, the lack of global magnetic field in Mars minimizes magnetic storms and the related processes. However, the patchwork ionosphere at the locations of regional magnetic fields may be affected by CME/shock impact. The solar wind has eroded the atmosphere of Mars considerably, and CME flow represents gusts of enhanced solar wind that modulate the continued erosion.
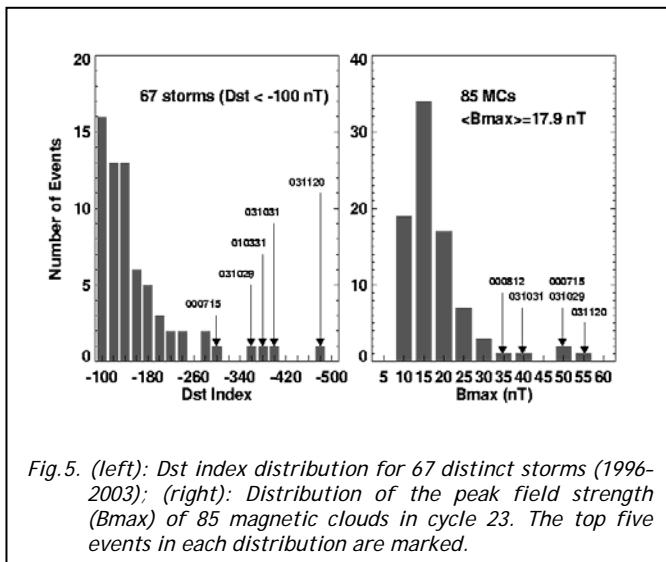

Fig. 5. (left): Dst index distribution for 67 distinct storms (1996-2003); (right): Distribution of the peak field strength (Bmax) of 85 magnetic clouds in cycle 23. The top five events in each distribution are marked.

Geomagnetic storms, measured by the Dst index, occur when ICMEs and CIRs containing southward magnetic field (Bs) arrive at Earth's magnetosphere resulting in magnetic reconnection with the geomagnetic field [see, e.g., 45]. The CIR-related storms

are more numerous, but they are seldom stronger than - 100 nT. The ICME related storms are infrequent and could reach a Dst of hundreds of nT. Fig. 5 shows the distribution of Dst for a all the storms in cycle 23 with Dst≤100 nT. All the superintense storms are associated with magnetic clouds carrying intense magnetic fields (Bmax). The Dst and Bmax ordering is not quite the same, because the Dst index is decided by additional factors such as the magnitude of Bs and the speed of MCs. For example, the intense storm on 2001 March 31 (Dst = - 387 nT) is not in Bmax distribution because the ICME was not an MC, but it had Bmax = 39 nT. Thus all ICMEs need to be considered for geoeffectiveness including the sheath ahead of them. Low-inclination MCs are sure to produce storms because they contain Bs either in the front or in the back of the clouds. However, the high-inclination MCs can produce extreme storms [46] when the axial field is southward or no storm at all [47] when the axial field is northward.

CME-driven shocks

Shock generation is an important aspect of the CMEs in the heliosphere. Most of the IP shocks detected at 1 AU are due to fast and wide CMEs. Occasionally, CIR-related shocks are also observed. Sometimes shocks are observed with no ICME (driver gas) behind them, but these are associated with CMEs ejected at large angles to the Sun-Earth line, so just the shock flanks (not the ICMEs) are intercepted by Earth. Shocks observed at 1 AU continue to be driven by the associated ICMEs [48]. This is demonstrated by the close correlation between shock speed and MC speed for 56 pairs observed during cycle 23. The correlation coefficient is very high (r=0.95).
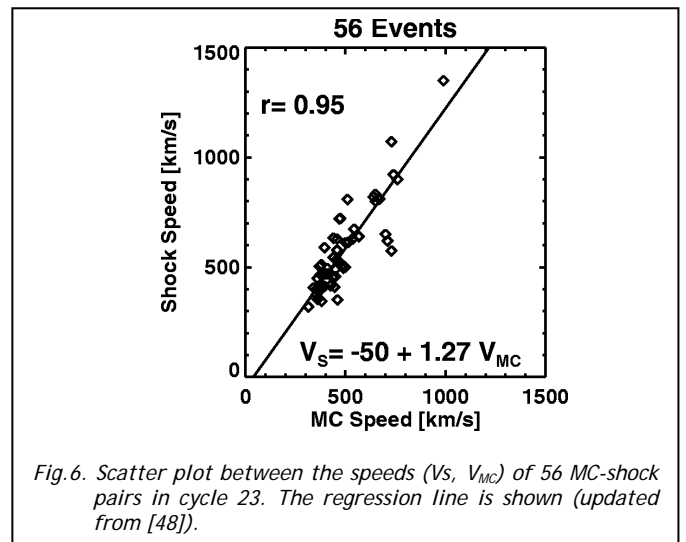

Fig. 6. Scatter plot between the speeds (Vs, V$_{MC}$) of 56 MC-shock pairs in cycle 23. The regression line is shown (updated from [48]).

Close to the Sun, CME-driven shocks are inferred from type II radio bursts. Within about 1 R$\odot$ from the solar surface, type II radio bursts occur at meter wavelengths and are observed by ground-based radio telescopes. The Radio and Plasma Wave (WAVES) experiment on board the Wind spacecraft observes radio emission at longer wavelengths (from decameter-hectometric or DH to kilometric wavelengths) corresponding to heliocentric distances of ~2 - 214 R$\odot$. Since the frequency of radio emission is decided by the plasma frequency in the

corona/IP medium, type II bursts at very low frequencies (very long wavelengths) correspond to large distances from the Sun. Very fast CMEs (high energy CMEs) result in type II radio bursts at all wavelengths from metric to kilometric (mkm). On the other hand, CMEs associated with purely metric type II bursts have the lowest speed (~600 km/s). CMEs associated with DH type II bursts are of intermediate speed. Of course, CMEs associated with type II bursts in general have kinetic energy larger than that of the general population.

Table 1 shows the progressive increase in speed, width and deceleration of CMEs associated with metric, DH, mkm type II bursts [49]. The large fraction of halo CMEs for mkm type II bursts reflects the fact that these CMEs are fast and wide. The increasing deceleration also reflects the fast and wide nature of mkm CMEs because of the drag force.

TABLE 1

Properties of CMEs associated with type II bursts

Property	All	m	DH	mkm	SEP	km
Speed (km/s)	487	610	1115	1490	1524	539
Width (deg)	45	96	139	171	182	80
Halos (%)	3.3	3.8	45.2	71.4	76	17.2
Acceleration (m/s^2)	-2	-3	-7	-11	-11	+3

The type II bursts confined to km wavelengths are due to accelerating CMEs, which do not produce shocks near the Sun, but attain sufficiently high speeds to drive shocks in the IP medium. Currently, the type II radio bursts is the primary means of tracking shocks (and hence CMEs) in the IP medium, apart from the interplanetary scintillation technique (see, e.g., [50]). While the Solar Mass Ejection Imager (SMEI) can image CMEs beyond LASCO field of view [51], the heliospheric imager (HI) on the STEREO mission can track CMEs over the entire Sun-Earth distance.

CMEs and SEPs

Each large solar energetic particle (SEP) event can be uniquely identified with a fast and wide CME at the Sun [12, 52]. The large SEP events are those with intensity >10 pfu (particle flux units) in the >10 MeV channel (1 pfu = 1 particle $cm^{-2}s^{-1}sr^{-1}$). Smaller and more numerous SEP events originate in flare reconnection regions. Direct evidence of particle acceleration by CME-driven shocks comes from the energetic storm particle (ESP) events in which the particles accelerated locally are detected when the shock arrives at the spacecraft. At this time the shock must have aged and weakened over a period ranging from less than a day to a couple of days in traversing the Sun-Earth distance. Near the Sun, the CME-driven shocks must be very strong, efficiently accelerating SEPs. However, CMEs do accelerate from rest, so they need time to attain a high enough speed before driving shocks. It turns out that SEPs are released when the CME reaches a height of a few R⊙ [53, 54].

CME-driven shocks take in what lies ahead of them, accelerate them and inject back into the heliosphere. Recent observations indicate that this so-called source

material is not just the ordinary solar wind: it is made up of ions from impulsive solar flares and previous gradual events, CIR events, pickup ions, CME ejecta, and the suprathermal tail of the solar wind [55]. In fact, CMEs associated with most of the large SEP events seem to be propagating through a medium disturbed and distorted by preceding CMEs, a process described as preconditioning [56, 57]. The scatter plot between CME speed and the SEP intensity in Fig. 7 shows that CMEs preceded by other wide CMEs most often result in high intensity compared to those not preceded by such CMEs.

SEP ions and electrons may suddenly have access to the inner magnetosphere during geomagnetic storms, where they can get trapped in a new radiation belt [58]. During the largest SEP events, the energetic protons can penetrate all the way to Earth's atmosphere leading to significant ozone depletion [59].

Fig. 8 compares the speeds of SEPeffective CMEs with those of the halo CMEs and geoeffective CMEs. Clearly the SEPeffective CMEs are the fastest. As shown in Table 1, the SEPeffective CMEs have properties similar to CMEs associated with mkm type II bursts. In fact there is a high degree of overlap between the sets of underlying CMEs. The only population that has a higher average speed (~2000 km/s) is the CMEs associated with ground level enhancement (GLE) in SEPs.
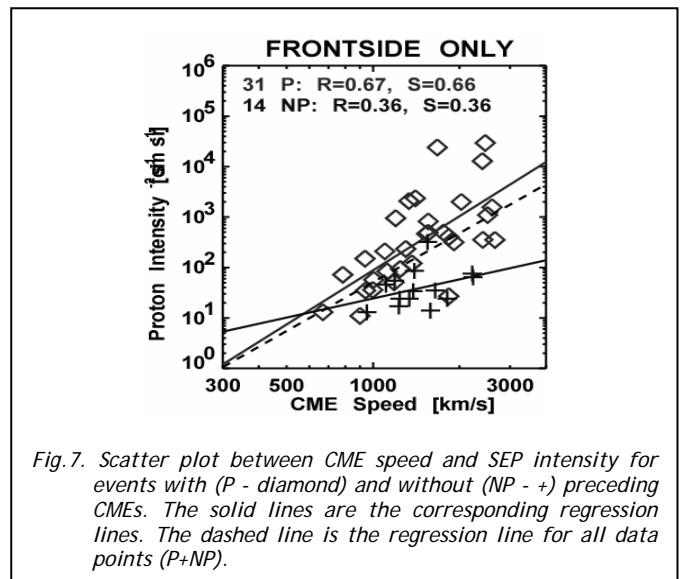

Fig. 7. Scatter plot between CME speed and SEP intensity for events with (P - diamond) and without (NP - +) preceding CMEs. The solid lines are the corresponding regression lines. The dashed line is the regression line for all data points (P+NP).
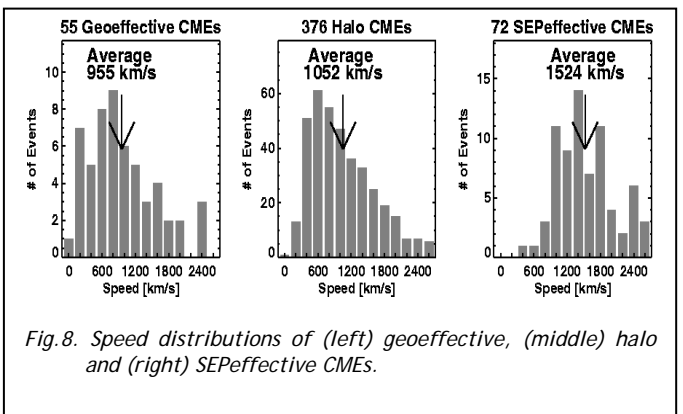

Fig. 8. Speed distributions of (left) geoeffective, (middle) halo and (right) SEPeffective CMEs.

Note that the average speeds of geoeffective and halo CMEs are similar. This is because the geoeffective CMEs form an approximate subset of the halo CMEs. The large discrepancy (factor of ~6) in the number of geoeffective and halo CMEs can be accounted for as follows. Only ~half of the halos are front-sided. Among the front side halos, only about a third are likely to originate close to the disk center (within a central meridian distance of 30 deg). This is an approximate subset because some partial halos can also be geoeffective and some full halos without southward component of the magnetic field may not be geoeffective.

CMEs and cosmic ray modulation

CMEs have been considered as the basic magnetic irregularities in the heliosphere that may be responsible for the 11-year variation in the galactic cosmic ray (GCR) intensity [60], the underlying mechanism being the same as Forbush decrease, but happening over the entire heliosphere. The hypothetical "propagating diffusive barriers" or PDBs having limited radial extent and moving with solar wind speed that have been invoked in modeling the GCR intensity over the solar cycle [61, 62]. CMEs could very well be these PDBs. Merged interaction regions, formed by the coalescence of interaction regions, shocks and ejecta, have also been thought to be PDBs. Global merged interaction regions (GMIRs) are shell-like structures (radial extent ~20 AU) of intense magnetic field encircling the Sun and extending to high latitudes beyond ~30 AU [63]. GMIRs have also been suggested as effective modulators of GCRs. CMEs do participate in MIRs and GMIRs along with shocks and stream interaction regions.

Ulysses observations suggest a picture of the inner and middle heliosphere as shown in Fig. 9 [64].
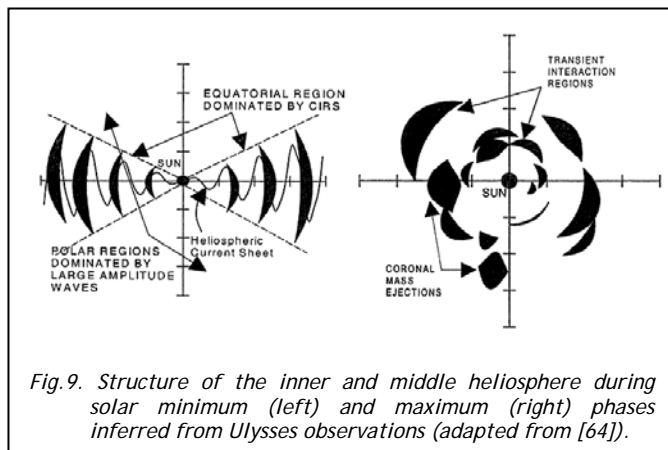

Fig. 9. Structure of the inner and middle heliosphere during solar minimum (left) and maximum (right) phases inferred from Ulysses observations (adapted from [64]).

During solar minimum, CIRs dominate in the equatorial regions. Of course, there must also be occasional ICMEs in the equatorial regions because the solar-minimum CME rate is ~0.5 per day. During the maximum phase, transient structures dominate all latitudes. It is not clear if this picture extends to the outer heliosphere. Presence of these transient structures at high latitudes is especially important because they can directly encounter and deflect GCRs entering the heliosphere along the polar directions. During one of the

best observed episodes of solar activity during October November 2003 [65], no GMIR was formed suggesting that true GMIRs may be quite rare structures [39]. In the absence of true GMIRs, one has to consider the effect of ICMEs at high latitudes for GCR modulation.

The solar polarity reversal occurs during solar maxima with the corresponding reversal of the heliospheric magnetic field.

The epoch when the north pole of the Sun has positive (negative) magnetic polarity is known as A>0 (A<0) epoch. The GCR intensity reaches a minimum during solar maxima and the recovery depends on what polarity the Sun's poles have. The recovery is sudden when the polarity reversal is from A>0 to A<0, while it is very gradual when the reversal is from A<0 to A>0, thus creating the characteristic flat-top + pointy profiles of GCR intensity. The influence of high-latitude CMEs has been proposed as a possible cause for such a pattern [3]. The GCR modulation by CMEs needs to be reinvestigated because of the increased CME rate recorded by SOHO and the large population of high-latitude CMEs during solar maxima. The high-latitudes CMEs are mainly important during A>0 epochs because GCRs enter the heliosphere from the polar regions. During A<0 epochs, the high-latitude CMEs are less important because the GCRs enter along the heliospheric current sheet (see Fig. 10).
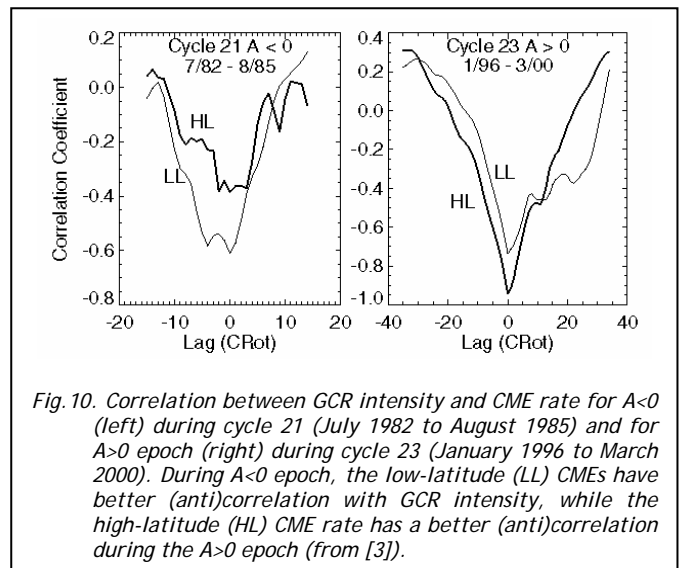

Fig. 10. Correlation between GCR intensity and CME rate for A<0 (left) during cycle 21 (July 1982 to August 1985) and for A>0 epoch (right) during cycle 23 (January 1996 to March 2000). During A<0 epoch, the low-latitude (LL) CMEs have better (anti)correlation with GCR intensity, while the high-latitude (HL) CME rate has a better (anti)correlation during the A>0 epoch (from [3]).

Summary and conclusions

We summarized the properties of various populations of CMEs and their consequences in the heliosphere. The population that is about to leave the coronagraphic field of view (~30 Ro) is clearly fast and wide and hence has a kinetic energy well above that of the general population. CMEs are responsible for the major disturbances in the heliosphere such as shocks, interplanetary ejecta, SEP events, interplanetary radio bursts, and large geomagnetic storms. CMEs associated with SEPs and mkm type II bursts are similar because the same shocks accelerate electrons and ions. CMEs associated with GLE events (a subset of large SEP events) are the fastest. CMEs responsible for geomagnetic storms

constitute an approximate subset of halo CMEs. All these special populations consist of energetic CMEs, which propagate far into the heliosphere. CMEs in the heliosphere are likely to participate in the modulation of galactic cosmic rays.

Solar cycle 23 witnessed the vast array of spaceborne and ground-based instruments that produced uniform and extended data sets on thousands of CMEs and their consequences in the heliosphere. These data sets enabled rapid progress in our understanding of the origin, propagation and heliospheric consequences of CMEs. Future research needs to address several key issues on CMEs. For geoeffectiveness and cosmic ray modulation, the magnetic field content in CMEs is important. Predicting the magnetic properties of CMEs based on solar observations is still far from reality. Understanding shock propagation in a highly inhomogeneous medium with various suprathermal particle populations needs to be properly understood. The issue of flux-rope structure of ICMEs needs to be resolved to effectively make use of remote-sensing observations of CMEs for predicting their heliospheric consequences. Combining theory and advanced modelling efforts with new data from Solar-B and STEREO is likely to make significant progress in addressing the unresolved issues.

Acknowledgement

REFERENCES

[1] S.W.Kahler, in: "Chapman Conference on Solar Eruptions and Energetic Particles", N.Gopalswamy and J. Torsti (Eds.), AGU GM, Washington DC, 2006, in press.

[2] G.E.Brueckner, "The Large Angle Spectroscopic Coronagraph LASCO", Solar Phys., Vol. 162, 1995, pp. 357–402.

[3] N.Gopalswamy, "A Global Picture of CMEs in the Inner Heliosphere", in: "The Sun and the Heliosphere as an Integrated System", G. Poletto and S. T. Suess (Eds.), Kluwer, Boston, Chapter 8, 2004, p. 201.

[4] R.A.Howard, D.J.Michels, N.R.Sheeley, Jr., M.J.Koomen, "The Observation of a Coronal Transient Directed at Earth", Astrophys. J., Vol. 263, 1982, L101.

[5] N.Gopalswamy, S.Yashiro, M.L.Kaiser, R.A.Howard, J.-L. Bougeret, "Characteristics of Coronal Mass Ejections Associated With Long-Wavelength Type Ii Radio Bursts", J. Geophys. Res., Vol. 106, 2001, p. 29219.

[6] P.J.Cargill, "On the Aerodynamic Drag Force Acting on Interplanetary Coronal Mass Ejections", Solar Phys., Vol. 221, 2004, p.135.

[7] B.Vrsnak, D.Ruzdjak, D.Sudar, N.Gopalswamy, Astron. Astrophys., Vol. 423, 2004, p. 717.

[8] N.Gopalswamy, A.Lara, S.Yashiro, R.A.Howard, "Coronal Mass Ejections and Solar Polarity Reversal", Astrophys. J., Vol. 598, 2003, L63.

[9] J.B.Smith, Jr., D.M.Speich, R.M.Wilson, E.Tandberg-Hanssen, S.T.Wu, "Prominence Mass Ejections and Their Effects on the Corona. I - the Eruptive Prominence of 21 August 1973 and the Surge of 4 December 1973", Solar Phys., Vol. 52, 1977, p. 379.

[10] H.-M.Wang, N.R.Sheeley, Jr., "Observations of Core Fallback during Coronal Mass Ejections", Astrophys. J., Vol. 567, 2002, p. 1211.

[11] N.Gopalswamy, M.Shimojo, W.Lu, S.Yashiro, K.Shibasaki, R.A. Howard, "Prominence Eruptions and Coronal Mass Ejection: A Statistical Study Using Microwave Observations", Astrophys. J., Vol. 586, 2003, p. 562.

[12] D.V.Reames, "Particle Acceleration at the Sun and in the Heliosphere", Space Sci. Rev., Vol. 90, 1999, p. 413.

[13] J.T.Gosling, D.J.McComas, J.L.Phillips, S.J.Bame, "Geomagnetic Activity Associated With Earth Passage of Interplanetary Shock Disturbances and Coronal Mass Ejections", J. Geophys. Res., Vol. 96, 1991, p. 731.

[14] M.Neugebauer, R.Goldstein, "Particle and Field Signatures of Coronal Mass Ejections in the Solar Wind", in: "Coronal Mass Ejections", Geophys. Monogr. Ser., vol. 99, N. Crooker, J. A. Joselyn and J. Feynman (Eds.), AGU, Washington DC, 1997, p. 245.

[15] J.Hirshberg, S.J.Bame, E.E.Robbins, "Solar Flares and Helium Enrichments", Solar Phys., Vol. 23, 1972, p. 467.

[16] H.G.Borrini, J.T.Gosling, S.J.Bame, W.C.Feldman, "Helium Abundance Enhancements in the Solar Wind", J. Geophys. Res. Vol. 87, 1982, p. 7370.

[17] L.F.Burlaga, E.Sittler, F.Mariani, R.Schwenn, "Magnetic Loop Behind an Interplanetary Shock: Voyager, Helios, and IMP-8 Observations", J. Geophys. Res., Vol. 86, 1981, p. 6673.

[18] R.P.Lepping, C.-C.Wu D.B.Berdichevsky, "Automatic Identification of Magnetic Clouds and Cloud-Like Regions at 1 Au: Occurrence Rate and Other Properties", Ann. Geophysica, Vol. 23, 2005, p. 2687.

[19] L.F.Burlaga, et al., "A Magnetic Cloud and a Coronal Mass Ejection", Geophys. Res. Lett., Vol. 9, 1982, p. 1317.

[20] N.Gopalswamy, et al., "The Pre-CME Sun", Space Sci. Rev., 2006, in press.

[21] T.Henke, et al., "Differences in the O7+/O6+ Ratio of Magnetic Cloud and Noncloud Coronal Mass Ejections", Geophys. Res. Lett., Vol. 25, 1998, p. 3465.

[22] S.T.Lepri, T.H.Zurbuchen, L.A.Fisk, I.G.Richardson, H.V.Cane, G.Gloeckler, "Fe Charge Distributions as an Identifier of Interplanetary Coronal Mass Ejections", J. Geophys. Res., Vol. 106, 2001, p. 29, 23.

[23] A.Reinard, "Comparison of Interplanetary CME Charge State Composition with CME-associated Flare Magnitude", Astrophys. J., Vol. 620, 2005, p. 501.

[24] A.B.Galvin, "Minor Ion Composition in CME-Related Solar Wind, in: "Coronal Mass Ejections", N. Crooker, J. A. Joselyn, J. Feynman (Eds.), AGU, Washington DC, 1997, p. 253.

[25] L.Klein, L.F.Burlaga, "Interplanetary Sector Boundaries 1971–1973", J. Geophys. Res., Vol. 85, 1980, p. 2269.

[26] P.Riley, C.Schatzman, H.V.Cane, I.Richardson, N.Gopalswamy, "On the Rates of Coronal Mass Ejections: Remote Solar and In Situ Observations", 2006, in press.

[27] C.C.Wu, R.P.Lepping, N.Gopalswamy, "Relationship among Magnetic Clouds, CMEs, and Geomagnetic Storms", Solar Phys., 2006, in press.

[28] N.Gopalswamy, "Properties of Interplanetary Coronal Mass Ejections", Space Sci. Rev., 2006, in press.

[29] R.P.Lepping, D.Berdichevski, "Interplanetary Magnetic Clouds: Sources, Properties, Modeling and Geomagnetic Relationship", Recent. Res. Geophysics., Vol. 3, 2000, p. 77.

[30] K.I.Paularena, C.Wang, R. von Steiger, B.Heber, "An ICME Observed by Voyager 2 at 58 AU and by Ulysses at 5 AU", Geophys. Res., Vol. 28, 2001, p. 2753.

[31] C.Wang, D.Du, J.D.Richardson, "Characteristics of Interplanetary Coronal Mass Ejections in the Heliosphere between 0.3 and 5.4 AU", J. Geophys. Res., Vol. 110, 2005, A10107.

[32] N.R.Sheeley, R.A.Howard, M.J.Koomen, D.J.Michels, R. Schwenn, K.-H.Muhlhauser, H.Rosenbauer, "Coronal Mass Ejections and Interplanetary Shocks", J. Geophys. Res., Vol. 90, 1985, p. 163.

[33] G.M.Lindsay, J.G.Luhmann, C.T.Russell, J.T.Gosling, "Relationships between Coronal Mass Ejection Speeds From Coronagraph Images and Interplanetary Characteristics of Associated Interplanetary Coronal Mass Ejections", J. Geophys. Res., Vol. 104, 1999, p.12, 515.

[34] N.Gopalswamy, et al., "Effective Interplanetary Acceleration of Coronal Mass Ejections", Geophys. Res. Lett., Vol. 27, 2000, p.145.

[35] R.Schwenn, A. dal Lago, E.Huttunen, W.D.Gonzalez, "The Association of Coronal Mass Ejections with Their Effects near the Earth", Ann. Geophysica, Vol. 23, 2005, p. 625.

[36] N.Gopalswamy, et al., "Radio signatures of coronal mass ejection interaction: Coronal mass ejection cannibalism?", Astrophys. J., Vol. 548(1), 2001, L91.

[37] N.Gopalswamy, "Coronal Mass Ejections: Initiation and Detection", Adv. Space Res., Vol. 31(4), 2003, p. 869.

[38] L.F.Buralaga, et al., "A Magnetic Cloud Containing Prominence Material - January 1997", J. Geophys. Res., Vol. 103, 1998, p. 277.

[39] J.D.Richardson, C.Wang, J.C. Kasper, Y.Liu, "Propagation of the October/November 2003 CMEs through the Heliosphere", Geophys. Res. Lett., Vol. 32, 2005, L03S03.

[40] B.Vrsnak, N.Gopalswamy, "Influence of the Aerodynamic Drag on the Motion of Interplanetary Ejecta", J. Geophys. Res., Vol. 107, 2002, SSH 2-1, CiteID 1019.

[41] N.Gopalswamy, A.Lara, S.Yashiro, M.L.Kaiser, R.A.Howard, "Predicting the 1-AU Arrival Times of Coronal Mass Ejections", J. Geophys. Res., Vol. 106(A12), 2001, pp. 29,207-29,218.

[42] N.Gopalswamy, A.Lara, P.K.Manoharan, R.A.Howard, "An Empirical Model to Predict the 1-AU Arrival of Interplanetary Shocks", Adv. Space Res., Vol. 36(12), 2005, p. 2289.

[43] L.F.Burlaga, "Interplanetary Magnetohydrodynamics", Oxford Univ. Press, New York, 1995.

[44] L.F.Burlaga, N.F.Ness, E.C.Stone, F.B.McDonald, J.D. Richardson, "Voyager 2 Observations Related to the October-November 2003 Solar Events", Geophys. Res. Lett., Vol. 32, 2005, L03S05.

[45] B.T.Tsurutani, W.D.Gonzalez, "The Interplanetary Causes of Magnetic Storms, in Magnetic Storms," Geophys. Monogr. Ser., Vol. 98, B. T. Tsurutani et al. (Eds.), AGU, Washington DC, 1997, p. 77.

[46] N.Gopalswamy, et al., "Solar Source of the Largest Geomagnetic Storm of Cycle 23", Geophys. Res. Lett., Vol. 32, 2005, p. 12.

[47] V.Yurchyshyn, H.Wang, P.R.Goode, Y.Deng, "Orientation, of the Magnetic Fields in Interplanetary Flux Ropes and Solar Filaments", Astrophys. J., Vol. 563, 2001, p. 381.

[48] N.Gopalswamy, A.Lara, P.K.Manoharan, R.A.Howard, Adv. Space Res., Vol. 36 (12), 2005. p. 2289.

[49] N.Gopalswamy, E.Aguilar-Rodriguez, S.Yashiro, S.Nunes, M.L. Kaiser, R.A.Howard, "Type II Radio Bursts and Energetic Solar Eruptions", J. Geophys. Res., Vol. 110, 2005, p. A12S07.

[50] P.K.Manoharan, "Evolution of Coronal Mass Ejections in the Inner Heliosphere: A Study Using White-Light and Scintillation Images", Solar Phys., Vol. 235, 2006, p. 345.

[51] D.F.Webb, J.C.Johnston, R.R.Radick, and the SMEI Team, "The Solar Mass Ejection Imager (SMEI): A New Tool for Space Weather", EOS, Trans. AGU, Vol. 83, 2002, p. 33.

[52] N.Gopalswamy, "Solar and Geospace Connections of Energetic Particle Events", Geophys. Res. Lett., Vol. 30(12), 2003, p. 8013.

[53] S.W.Kahler, "Injection Profiles of Solar Energetic Particles as Functions of Coronal Mass Ejection Heights", Astrophys. J., Vol. 428, 1994, p. 837.

[54] N.Gopalswamy, H.Xie, S.Yashiro, I.Usoskin, "Coronal Mass Ejections and Ground Level Enhancements in: Proc. 29th Intern. Cosmic Ray Conf., Pune, India, Vol. 2, 2005, pp. 169-172.

[55] R.Mewaldt et al., in: "Chapman Conference on Solar Eruptions and Energetic Particles", N. Gopalswamy, R. Mewaldt, and J. Torsti (eds), AGU GM, Washington DC, 2006, in press.

[56] N.Gopalswamy, et al., "Large Solar Energetic Particle Events of Cycle 23: a Global View", Geophys. Res. Lett., Vol. 30(12), 2003, p. 8015.

[57] N.Gopalswamy, S.Yashiro, S.Krucker, G.Stenborg, R.A.Howard, "Intensity Variation of Large Solar Energetic Particle Events Associated With Coronal Mass Ejections", J. Geophys. Res., Vol. 109, 2004, p. A12105.

[58] K.R.Lorentzen, J.E.Mazur, M.D.Looper, J.F.Fennell, J.B. Blake, "Multisatellite Observations of MeV Ion Injections During Storms", J. Geophys. Res., Vol. 107(A09), 2002, p. 1231.

[59] C.H. Jackman, et al., "Neutral Atmospheric Influences of the Solar Proton Events in October-November 2003", J. Geophys. Res., Vol. 110, 2005, p. A09S27.

[60] G.Newkirk, A.J.Hundhausen, V.Pizzo, "Solar Cycle Modulation of Galactic Cosmic Rays - Speculation on the Role of Coronal Transients", J. Geophys. Res., Vol. 86, 1981, p. 5387.

[61] F.B.McDonald, J.H.Trainor, N.Lal, M.A.I. van Hollebeke, W.R. Webber, "The Solar Modulation of Galactic Cosmic Rays in the Outer Heliosphere", Astrophys. J., Vol. 249, 1981, p. L71.

[62] J.S.Perko, L.A.Fisk, "Solar Modulation of Galactic Cosmic Rays. V - time-dependent modulation, J. Geophys. Res., Vol. 88, 1983, p. 9033.

[63] L.F.Burlaga, F.B.McDonald, N.F.Ness, R.Schwenn, A.J.Lazarus, F.Mariani, "Interplanetary Flow Systems Associated With Cosmic Ray Modulation in 1977-1980", J. Geophys. Res., Vol. 89, 1984, p. 6579.

[64] A.Balogh, "The evolving Sun and its Influence on Planetary Environments", B. Montosinos, A. Gimenez, E.F. Guinan (Eds.), ASP Conf. Ser., Vol. 269, 2002, p. 37.

[65] N.Gopalswamy, L.Barbieri, E.W.Cliver, G.Lu, S.P.Plunkett, R. M.Skoug, "Introduction to Violent Sun-Earth Connection Events of October-November 2003", J. Geophys. Res., Vol.110, 2005, p. A09S00.